

NPS ARCHIVE
1959
EATON, W.

DESIGN AND CONSTRUCTION OF
INSTRUMENTATION FOR INVESTIGATING
THE OPTICAL DISPERSION OF GASES
BY INFRARED INTERFEROMETRY

WILLIAM G. EATON
AND
FREDERICK E. THOMAS

LIBRARY
U.S. NAVAL POSTGRADUATE SCHOOL
MONTEREY, CALIFORNIA

DESIGN AND CONSTRUCTION OF INSTRUMENTATION
FOR INVESTIGATING
THE OPTICAL DISPERSION OF GASES BY
INFRARED INTERFEROMETRY

* * * * *

William G. Eaton

and

Frederick H. Thomas

DESIGN AND CONSTRUCTION OF INSTRUMENTATION
FOR INVESTIGATING
THE OPTICAL DISPERSION OF GASES BY
INFRARED INTERFEROMETRY

by

William G. Eaton

Lieutenant Commander, United States Navy

and

Frederick H. Thomas

Captain, United States Air Force

Submitted in partial fulfillment of
the requirements for the degree of

MASTER OF SCIENCE
IN
PHYSICS

United States Naval Postgraduate School
Monterey, California

1959

NPS ARCHIVE
1959
EATON, W.

Thesis

DESIGN AND CONSTRUCTION OF INSTRUMENTATION
FOR INVESTIGATING
THE OPTICAL DISPERSION OF GASES BY
INFRARED INTERFEROMETRY

by

William G. Eaton

and

Frederick H. Thomas

This work is accepted as fulfilling
the thesis requirements for the degree of

MASTER OF SCIENCE

IN

PHYSICS

from the

United States Naval Postgraduate School

ABSTRACT

The design and construction of a modified Rayleigh Interferometer and allied systems was undertaken at the U. S. Naval Postgraduate School by Lieutenant Commander William G. Eaton, USN, and Captain Frederick H. Thomas, USAF.

The inherent weakness of low radiation intensity associated with Rayleigh type interferometers, especially in the infrared region, when measuring the refractive indices of gases led to the design and construction of a multi-chambered refractometer. The theory of this design was based on the gain in intensity achieved by multiple slit interferometry.

Optical components, capable of allowing investigation in the infrared region between one and 25 microns, were installed in the optical system. The vacuum and gas admission system, which provides a pressure differential of at least one atmosphere, incorporates fractional distillation for gas purification.

Time limitations prohibited an actual determination of the index of refraction of a gas with this system, however, it is hoped that future investigations will be made utilizing this instrumentation, and that the results justify the theoretical forecast.

We wish to express our appreciation to Professor Sydney H. Kalmbach for allowing us to capitalize on an idea of his conception and for his guidance during all phases of the project. We also wish to acknowledge, with appreciation, the technical advice and assistance obtained from Mr. M. K. Andrews, Mr. R. C. Moeller, Mr. K. C. Smith, and Chief Opticalman A. N. Goodall, USN.

TABLE OF CONTENTS

Section	Title	Page
1.	Introduction	1
2.	Theory of Dispersion in Gases	1
3.	Interferometric Determination of Index of Refraction	3
4.	The Advantage of a Multiple Channel Interferometer	4
5.	General Description of Instrumentation	5
6.	Modified Rayleigh Interferometer	6
7.	Gas and Vacuum System	9
8.	Optical System	9
9.	Recording Components	11
10.	System Checks and Alignment	12
11.	Conclusions	13
12.	Recommendations	15
13.	Bibliography	17
14.	Appendix I	18
15.	Appendix II	21
16.	Appendix III	23
17.	Appendix IV	26

LIST OF ILLUSTRATIONS

Figure	Page
1. Detector Slit Width Determination	18
2. Divergence of Energy Due to Exit Slit Width	21
3. Effect of Divergence of Energy in Interferometer Channel	22
4. Phase Relationships of Three Alternate Slits	24
5. Phase Relationship of Alternate Groups of Three Slits	25
6. Infrared Source and Monochromator	26
7. Interferometer Optical System	27
8. Vacuum and Distillation System	28
9. Modified Rayleigh Interferometer and Associated Components	29
10. Composite System with Light Covers Removed	30
11. Composite System with Light Covers Installed	31



* TABLE OF SYMBOLS

n	Index of Refraction
ω_i	i^{th} Characteristic Frequency of Gas Molecule
ω	Frequency of Incident Light Wave
N_i	No/Unit Volume of Oscillators of Characteristic Frequency ω_i
m_i	Mass of i^{th} Oscillator
F	Fringe Count
λ	Wave Length
T	Temperature $^{\circ}\text{K}$
ΔP	Pressure Differential, Gas-Vacuum
L	Geometrical Length of Interferometer
I	Intensity
β	$\frac{1}{2}$ Phase Difference Across Slit of Width a, $\beta = \frac{\pi a \sin \theta}{\lambda}$
γ	$\frac{1}{2}$ Phase Angle of Adjacent Slits, $\gamma = \frac{\pi d \sin \theta}{\lambda}$
N	Number of Slits
d	Slit Distance, Distance Between Centers of Adjacent Slits
θ	Angle Between the Plane of the Slit and the Normal to the Incident Radiation
m	Integral Number 0, 1, 2, 3, etc.
s	Detector Slit Width
f	Focal Length of Paraboloidal Mirror
$\delta \theta$	Angular Halfwidth of Principal Maximum
a	Width of Interference Slit
w	Distance, Edge of Mask Slit to Side of Channel
D	Width of Channel



g Exit Slit Width

R Resultant Amplitude of Six Slits

R_1 Resultant Amplitude of One Set of Alternate Slits

R_2 Resultant Amplitude of Second Set of Alternate Slits

R_o Amplitude Contribution of One Slit

ϕ Phase Difference



1. Introduction

The optical dispersion of gases by interferometric means has long been a subject of interest and investigation. However, the majority of investigations of this phenomenon have been largely confined to the region of visible light. The purpose of our investigation was to design and construct an interference refractometer and associated components which would provide determinations of the index of refraction of gases in the one to 25 micron region of the infrared spectrum.

O'Leary and Lauterbach [2] using a gas interferometer designed and constructed by Engle and Pederson [1] investigated the optical dispersion of ammonia gas in the one to three micron region of the infrared spectrum. The design and construction of our system was undertaken to (1) overcome the weak diffraction pattern they encountered, which is a major difficulty with this type of refractometer, by increasing the radiation intensity delivered to the detector and (2) to extend the range of investigation by installing optical components and a suitable detector in the system which will permit operation to the limit of the available monochromator. The methods decided upon to accomplish these goals are discussed in later sections.

2. Theory of dispersion in gases

Gas molecules, consisting of atoms carrying positive and negative charges, can be considered an assemblage of oscillating dipoles emitting electromagnetic radiation characterized by one or more natural frequencies of oscillation. A molecule containing N atoms has $3N-6$ ($3N-5$ if the molecule is linear) kinds of motion and associated with each kind is a characteristic vibrational frequency. As long as the vibrations are not

violent they are essentially harmonic. [4].

When electromagnetic radiation passes through gas, the varying electric fields of the incident waves impress forced vibrations upon the gas molecules. Therefore, the resultant motion (oscillations) of a gas molecule can be considered as due to an elastic restoring force (responsible for the free oscillations), a frictional force (responsible for the damping), and an external sinusoidal force (due to the electric field of the incident wave). The electromagnetic waves at any point in a gaseous medium result from the combined effects of the incident waves and the secondary waves radiated by the molecule undergoing forced oscillations. [3]

The frequency dependence of the index of refraction, known as dispersion, can be expressed by the following formula, developed for ω appreciably different from ω_{oi} ,

$$n^2 = 1 + \frac{e^2}{\epsilon_0} \sum \frac{N_i/m_i}{\omega_{oi}^2 - \omega^2} \quad [3]$$

and illustrates normal dispersion, i.e., when n gradually increases with increasing frequency.

However, for any investigation made in the infrared region particular attention must be paid to the fact that the wave number range covered by molecular vibration is approximately 100 to 5000 cm^{-1} which means that the wave length range is two to 100 microns [4]. The number of characteristic frequencies encountered depends on the gas in use. When the frequency of the incident wave approaches the characteristic frequency, the behavior of the index of refraction departs from that of



normal dispersion and exhibits what is known as anomalous dispersion. First as ω approaches ω_0 the index of refraction rises rapidly, decreases as ω passes through ω_0 to a low value, and then increases again to a normal value. Except for the molecular damping force, although it is usually small in gases, the value of n as forecast by the previously mentioned formula would increase to infinity. Also occurring when ω approaches ω_0 is the phenomenon known as resonance absorption with peak value at $\omega = \omega_0$. This occurs when the amplitude of the forced molecular oscillations reach their maximum value and strong absorption is exhibited as the energy of the incident wave is transferred to the oscillating molecules.

For the interested reader a detailed treatment of molecular structure may be found in Harrison, Lord, and Loofbourow [4] and an excellent development of the dispersion theory may be found in Rossi [3].

3. Interferometric determination of index of refraction.

An interferometer, by dividing a beam of monochromatic light from a point source into two or more parts then rejoining the divided beam to form interference fringes, provides a means for determining the refractive index of gases. By causing the beam to split, and travel in different media with the same geometrical path length, it is possible to measure the optical path difference by interpretation of the variations in the interference fringe patterns. One of the more accurate means of determining refractive indices of gases is by use of the Rayleigh interferometer. [6]

The modified Rayleigh interferometric system, built by the writers, was designed to provide measurement of the index of refraction of a gas with respect to a vacuum. This is accomplished by passing one part of the beam through evacuated chambers, while the other part of the beam is

passed through chambers to which gas is admitted at a controlled rate. The change in gas pressure (density) alters the optical path and a shift in the fringe pattern position occurs. To an observer, this shift appears as a steady movement of maxima (or minima) as pressure is gradually changed. If the fringes are counted for a given change in pressure the index of refraction at a specific wave length may be calculated by the formula: [10]

$$n-1 = F \cdot \lambda \cdot \frac{T}{273} \cdot \frac{760}{\Delta P} \cdot \frac{1}{L}$$

This formula, suitably corrected for departure from the ideal gas law, provides a value of n corrected to standard temperature and pressure using vacuum as a standard medium.

4. The advantage of a multiple channel interferometer.

Candler [8] states "Low intensity is a major difficulty with this instrument," when describing the Rayleigh Interferometer. Thus any steps taken to improve the capability of the instrument must, of necessity, point toward a method of increasing the intensity of the radiation entering the interferometer or increasing the radiation reaching the detector. In our case, use of the Perkin-Elmer Infrared Spectrophotometer as an infrared source limits the intensity that is delivered to the interferometer, so the alternative of increasing the amplitude of the intensity of the interference maxima suggested itself as the logical starting point in designing an improved system.

The following equation shows the effect of Fraunhofer diffraction of N equally spaced slits of equal aperture upon intensity:

$$I = I_0 \frac{\sin^2 \beta}{\beta^2} \frac{\sin^2 N \gamma}{\sin^2 \gamma}$$

It is evident that for small values of the phase angle γ that $I \sim N^2$.

From this premise came the idea and subsequent design of an interferometer, whereby increased intensity would be gained by increasing the number of channels. The design and construction details of this modified Rayleigh interferometer are to be found in Section 6.

In order to maintain the proper phase relationship between radiation travelling separate channels in the gas and vacuum, and have it recombine to form proper minima and maxima, it was necessary to design the tube so that alternate chambers were provided for vacuum with the remaining in-between chambers allocated for the gas in question. Appendix III deals with the mathematical development of the phase relationships of radiation from alternate slits.

5. General description of instrumentation.

The system, illustrated in figures 6 through 11, and as designed specifically for the interferometric analysis of the index of refraction of gases, consists of the following essential components:

a. A Perkin-Elmer Infrared Spectrophotometer, Model 13, with KBr prism, utilized as (1) the source of infrared energy and (2) the means of selection of monocromatic wave lengths in the region of the spectrum being investigated.

b. A modified version of the Rayleigh refractometer utilizing six



energy transmitting channels or tubes instead of two. A more detailed description of this follows in Section 6.

c. A vacuum system capable of sustaining a vacuum of one micron of Hg for a period of two minutes with the pump secured and with the facility of permitting alternate channels of the refractometer to be evacuated as desired.

d. A gas system closely allied with the vacuum system which permits admission of the gas under investigation into the channels, alternate to those under vacuum, of the refractometer.

e. An optical system for directing the infrared energy from the monochromator through the refractometer to the energy detector.

f. A pressure differential measuring system consisting of a mercury manometer gauge capable of registering a pressure differential of slightly greater than one atmosphere and a cathetometer equipped with a vernier capable of reading directly to tens of microns.

g. A copper-constantan thermocouple and associated potentiometer for determining the temperature of the refractometer during the period data is being obtained.

h. A thermocouple detector containing a KBr window, highly sensitive to infrared radiation.

i. A Leeds and Northrup Speedomax Recorder, Type G, for the continuous graphical presentation of energy received by the detector.

6. Modified Rayleigh interferometer.

In the matter of terminology, the modified Rayleigh interferometer will be referred to interchangeably as a refractometer, an interferometer or tube. A detailed photograph of this instrument is included herein as figure 9.



The interferometer has basic dimensions as follows:

Length	49.520 cm	
Width	5.897 cm	outside
	3.377 cm	inside
Height	5.940 cm	outside
	3.427 cm	inside
Channel width	0.478 cm	
Partition width	0.102 cm	

This interferometer is the heart of our system and was designed and fabricated by the writers for the purpose of this and/or future investigation. A description of the theory of operation of this instrument is contained in Section 3.

The sides, top and bottom of the instrument are basically one half inch thick brass plates, cut to size, milled with slots for the five channel partitions and dovetailed at the corners to provide a smooth, tight fit. The partitions are of thin brass sheet 1.02 mm thick extending for the full length of the tube. The dovetail joints and the partitions were silver soldered together with 430 silver solder to give as tight a seal as possible. After soldering, the ends of the tube were machined parallel and polished smooth.

On the top plate, two groups of three slots were cut completely through the brass. Each group opens to alternate channels. Over the top of each group of slots a brass manifold, topped by a vacuum coupling connector for receiving a glass tube, was secured by screws and made vacuum tight by a neoprene gasket.



Five coats of Glyptal enamel were baked on the interior and two coats of the same on the exterior.

At either end, flanges were attached to the tube by screws. These flanges serve the purpose of securing in place a spring loaded disc which hold the special windows that seal each end of the tube. The end windows mounted for this investigation are of KBr, six mm thick and 55 mm in diameter. It can be noted here that the size of these windows was the limiting factor in determining the size, and thereby the number of channels, of the interferometer. The KBr windows were sealed against the end of the tube with a thin latex rubber gasket, lightly coated with silicon vacuum grease, giving a vacuum seal around the circumference of the window and along the partitions. Several other methods of sealing the end windows were attempted, including (1) dissolving Apiezon W-40 vacuum wax in benzene and applying this to the end of the tube, (2) heating Apiezon W-40 vacuum wax and applying as in (1), and (3) the use of neoprene gaskets. The Apiezon wax seals satisfactorily, but is quite messy and liable to smear on the window. A word of caution in using heat near the windows is in order as these crystals are extremely susceptible to crackage from direct heat. The neoprene gaskets, due to thickness, were subject to blow-through between channels.

A thin metal mask with slits four mm wide and six mm between slit centers was fitted over one end to provide the proper interference pattern. (See Appendix II for slit width determination).

When mounted for operation the tube is held in special mountings permitting vertical and lateral adjustments.



7. Gas and vacuum system.

This system was designed with simplicity and flexibility foremost in mind. It is an integrated system in which vacuum or pressure can be applied as desired to either manifold of the interferometer. The entire system is illustrated schematically in figure 8 and photographically in figures 10 and 11. The glass tubing is one half inch diameter pyrex. All auxiliary glass apparatus such as stopcocks, stoppers and traps are of high vacuum design and also made of pyrex glass. Flexible rubber vacuum hose was utilized in connections to the interferometer and to the vacuum pump. The pump, a Duo Seal Vacuum Pump, maintains a vacuum slightly below one micron. One trap cooled by liquid air was placed in the system just ahead of the vacuum pump to rid the system of contaminants and to collect used gas after completion of an experimental run. Near this same position a stopcock is installed for either venting the system or for providing a vacuum take-off to a Pirani gauge. By proper placement of the bank of four stopcocks, vacuum can be placed on either side of the mercury manometer and to either manifold of the interferometer.

The gas to be investigated will be admitted to the system under pressure and allowed to flow immediately to a liquid air trap where it can be purified by fractional distillation. By careful manipulation of the liquid air container it can be admitted to the system at a controlled rate. The proper placement of stopcocks permits the gas to flow to either side of the manometer tube and interferometer, the other side remaining evacuated.

8. Optical system.

As shown in figures 6, 7, 9, and 10, the optical system consists of (1) source slit, which is actually the exit slit of the monochromator,



(2) a 14° off-axis paraboloidal mirror for directing parallel rays of energy through the interferometer via a plane mirror necessary for reversing direction, (3) the interferometer, (4) a second 14° off-axis paraboloidal mirror for focusing the interference pattern at the detector slit, (5) the detector slit set in width for receiving one interference fringe at a time (see Appendix I for mathematical discussion of slit width determination), (6) an ellipsoidal mirror for focusing the detector slit energy on the detector, and (7) the thermocouple detector with KBr window and matched preamplifier. Here again design centered around the need for simplicity, flexibility, accessibility and ease of alignment.

Two 120 cm optical benches equipped with traversing supports were used to support the optical system. The first paraboloidal mirror was mounted facing the exit slit of the monochromator. Since this resulted in the wrong direction for the flow of energy, a plane mirror was so placed as to reverse the energy toward the interferometer, which was mounted on one of the optical benches. The details of the interferometer have already been discussed in Section 6 and it need only be mentioned here as being a portion of the optical system.

For adjustment purposes, a specially designed support plate of $3/16"$ aluminum was mounted on three traversing supports, two on one optical bench and the third on the other bench. The main purpose of this plate is to permit accurate alignment of the detector, ellipsoidal mirror, detector slit and the second 14° paraboloidal mirror. By traversing the support plate and pivoting the paraboloidal mirror, it is possible to quickly align the detector with the interferometer. The basic layout of the optical system enabled the removal of one mirror which had been



required in previous layouts and reduced the optical path to approximately 210 cm.

Provisions were made for mounting a prism and long focus microscope adjacent to the detector slit so that optical alignment in the visible range can be checked or established. Normally the green line of mercury is utilized for this by setting the wave length drum of the spectrophotometer at 2100. To insure protection against stray radiation the entire support plate and part of the interferometer is enclosed in an aluminum cover which is thoroughly blackened on the inside.

9. Recording components.

A Leeds and Northrup Speedomax, Type G recorder is to be utilized while taking data. This recorder receives its signal from the amplifier associated with the Mk 13 Spectrophotometer. The amplifier in turn is modulated by the preamplifier of the thermocouple detector. Maximum intensity of a fringe is amplified to cause maximum deflection of the pen.

A mercury manometer capable of indicating a maximum pressure differential of one atmosphere was installed with one arm attached to each manifold of the interferometer. Considerable care was taken in building and mounting the columns of mercury to insure an optically clear tube in the region where measurements of the menisci would be taken and to provide a strong support to prevent accidental breakage of the manometer. A cathetometer was mounted at the end of the optical benches (approximately 6° from the manometer) in such a position as to bring the sighting telescope in a line perpendicular to the plane of the manometer. Sightings of the menisci are facilitated by placing a light



background with dark diagonal lines behind the tube and at the same time shining a flashlight beam on the menisci. Readings with a direct accuracy of 10 microns are obtainable from the vernier of the cathetometer.

Measurement of the temperature of the interferometer is accomplished by a copper-constantan thermocouple, using a Rubicon Precision Potentiometer for measuring potential difference and a standard reference at 0° C. Conversion of the potential difference to temperature is made by use of standard tables.

10. System checks and optical alignment.

The initial system check of the Mk 13 Spectrophotometer was begun in August 1958 and continued for three months. A complete optical, electronic and mechanical alignment was performed during this period.

[12] This check and alignment resulted in the replacement of several component parts of the amplifier including a regohm regulator, renewal of the Nernst glower in the source system of the spectrophotometer and the complete adjustment of the slits and slit drive mechanism of the monochromator. The culmination of the checks, replacements and alignments was to compare maximum energy values as shown by the Speedomax with those listed in reference [12]. Several runs with the spectrophotometer in double beam operation were made in order to check the infrared absorption of various thin plastic films. These results compared closely to those found in the literature, thus indicating satisfactory operation of the spectrophotometer. For the investigation of gases the spectrophotometer was returned to single beam operation.



The alignment of the exterior optical system was accomplished with very little difficulty. The first paraboloidal mirror and its accompanying plane mirror were aligned by shining a beam of light backwards through the interferometer and focusing this on the exit of the monochromator. Next, with the mercury green line shining through the exit slit, the interferometer was aligned parallel to, and in the center of the energy beam. The second paraboloidal mirror was then focused on the detector slit and finally the ellipsoidal mirror was focused on the detector for maximum energy.

The final system check involved the vacuum system, and this proved most difficult of all. The glass tubing system, including stopcocks and traps, after initial fabrication, provided a minimum of trouble. However, the other portions of the system including the interferometer, rubber tubing and Pirani gauge connections proved worrisome to the point of distraction. These were a constant source of small leaks, difficult to find, and even more difficult to eliminate. The system was checked and rechecked until a vacuum-pressure differential between the two manifolds of the interferometer could be maintained at less than .1 mm of Hg in a three hour period.

Prior to making a run, the detector slit is to be set at the prescribed setting by use of a comparator (see Appendix I for this determination), and a final check of the interference pattern (utilizing the Hg green line) may be observed with the long focus microscope.

11. Conclusions.

Although lack of time prevented an actual index of refraction determination with the equipment to prove the success of theoretical design, the writers feel that future investigations using this system

will verify initial predictions. We also feel that the system will function with a high degree of accuracy and maximum alignment and operating ease due to "quality control" exercised in the construction process.

Based on the method of expected accuracy used by O'Leary and Lauterbach [2], we predict a reduction in relative error by a factor of five over their results through the use of this present interferometric system. The following error values are predicted for separate measurements:

1. Length of tube, where measurement of the length, 49.520 cm, was accurate to 0.001 inch

$$\frac{dL}{L} = \frac{0.001 \times 2.54}{49.520} = 0.005\%$$

2. Fringe count, with a change of 0.1 of a fringe detectable, over a range of 100 fringes

$$\frac{\Delta F}{F} = \frac{0.1}{100} = 0.001\%$$

3. Temperature, readable to 0.25°

$$\frac{dT}{T} = \frac{0.25}{300} = 0.083\%$$



4. Pressure differential, readable to 0.01 mm, over a range of 500 mm

$$\frac{d(\Delta P)}{\Delta P} = \frac{0.01}{500} = 0.002 \%$$

This results in an overall expected error of 0.09% in the determination of the index of refraction as related to the process of measuring the system variables.

12. Recommendations.

Future experimentation with the apparatus as assembled holds vast possibilities. With comparatively little effort a complete survey of different gases in the photoelectric infrared region (.75 μ - 3 μ) and the near infrared region (3 μ - 25 μ) can be made.

No change in the apparatus based on improved theoretical concepts is anticipated; however, there are several changes in the present physical setup which would, it is believed, create a more accurate and efficient investigation.

Where possible, reduce the length of the optical path. This may be done by moving the interferometer closer to the monochromator and by altering the support plate so as to bring the second paraboloidal mirror closer to the interferometer. It has also been suggested [2], and these writers concur, a Cassegrainian mirror placed at the exit slit of the monochromator would permit easier alignment with the interferometer and a shortening of the optical path.

Shock mountings of some description should be placed under the legs of all tables holding the experimental apparatus, in order that



undesirable vibrations caused by heavy exterior automotive traffic
be eliminated.

If it should be desirable to pursue the theory of this interferometer to one containing more than six channels, then larger windows would be needed. The experience gained from fabricating this interferometer indicates six channels are the maximum which can be practically made and still accomodate a 55 mm diameter window. Also, it would be highly desirable to have a quantity of, say six, end windows on hand as immediate replacements if such are needed.

The services of a Perkin-Elmer maintenance man should be available at least once a year to check the Mk 13 Spectrophotometer completely for optimum operation.

The feasibility of enclosing the entire apparatus in a gas tight container and then filling this container with a non infrared sensitive gas should be considered. This configuration would result in a much more stable system and would reduce the problem of vacuum leaks manyfold.



BIBLIOGRAPHY

1. R. K. Engle and D. M. Pederson, Design and Construction of Instrumentation for Investigating the Optical Dispersion of Ammonia Gas, U. S. Naval Postgraduate School, Monterey, California, 1951.
2. A. C. O'Leary, Jr. and W. R. Lauterbach, Interferometric Observations of the Optical Dispersion of Ammonia in the Near Infrared, U. S. Naval Postgraduate School, Monterey, California, 1958.
3. B. Rossi, Optics, Addison-Wesley Publishing Co., Inc., Reading, Mass., 1957.
4. Harrison, Lord and Loofbourow, Practical Spectroscopy, Prentice-Hall, Inc., New York, 1949.
5. R. W. Wood, Physical Optics, The Macmillan Co., New York, 1940.
6. W. E. Williams, Applications of Interferometry, Methuen and Co., Ltd., London, 1950.
7. J. W. Strutt, (Baron Rayleigh), Scientific Papers, Vol., V, Art. 339, Cambridge University Press, London, 1912.
8. C. Candler, Modern Interferometers, Hilger & Watts Ltd., Hilger Division, 1951.
9. F. A. Jenkins and H. E. White, Fundamentals of Optics, McGraw-Hill Book Co., Inc., New York, 1950.
10. J. K. Robertson, Introduction to Physical Optics, D. Van Nostrand Co., Inc., New York, 1942.
11. Instruction Manual, Perkin-Elmer Infrared Equipment, Vols. 1 & 2, The Perkin-Elmer Corp., Norwalk, Conn., 1952.
12. Model 13 Ratio Recording Infrared Spectrophotometer Operating and Maintenance Instructions, The Perkin-Elmer Corp., Norwalk, Conn., 1955.

APPENDIX I

Detector Slit Width Determination

The angle between interference principal maxima of a Rayleigh interferometer is given by the expression: [9]

$$d \sin \theta = m\lambda, \quad m=1$$

$$\text{for small angles } \sin \theta = \theta, \text{ so } d\theta = \lambda, \quad \theta = \frac{\lambda}{d}$$

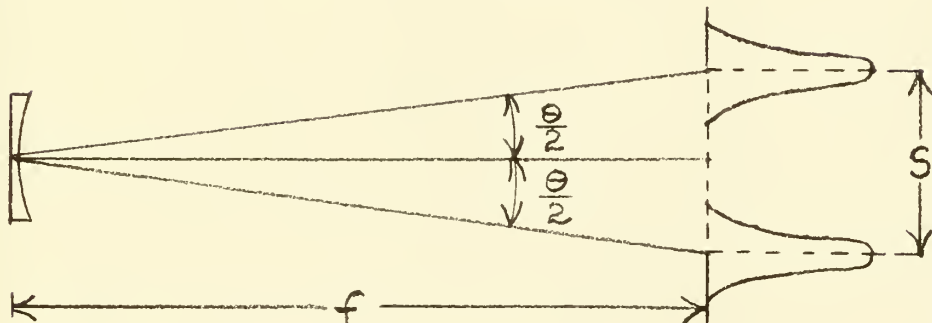


Figure 1. Detector Slit Width Determination

From the geometry of the optical path as seen in Figure 1,

$$\tan \frac{\theta}{2} = \frac{S/2}{f}$$

Again for small angles,

$$\frac{\theta}{2} = \frac{S/2}{f}$$

therefore, for the paraboloidal mirror with a focal length of 267 mm, and a slit center to center distance of 6 mm

$$S = \frac{\lambda F}{d} = \frac{267\lambda}{6} = 44.5\lambda$$

This would provide a maximum slit width which would always have the energy equivalent of one principal maxima present.

For closer analytical control, it would be more desirable to limit the size of the slit so that only one, or part of one particular principal maxima could possibly be in the slit at any time. This would lead to

$$S < \frac{44.5}{2} \lambda$$

or to an angular half width of principal maxima determination as follows: [9]

$$\delta\theta = \frac{\lambda}{A} = \frac{\lambda}{Nd \cos \theta}$$

again for small angles

$$\frac{\lambda}{6 \times 6 \times 1} = \frac{\lambda}{36}$$

For a focal length of 267 mm this results in a linear half width of

$$\frac{2 \times 267}{36} = 7.85\lambda$$

Total width of principal maxima is

$$2 \times 7.85\lambda = 14.7\lambda$$



Therefore, the optimum detector slit width should be between 14.7λ and 22.25λ . This range positively eliminates the possibility of any out of phase principal maxima appearing in the slit for an infinitely narrow exit slit of the monochromator. The need for a finite exit slit width alters the optimum detector slit width since allowances must be made for the additional fringes formed when the exit slit is opened a finite amount. A geometrical determination indicates that combinations of exit and detector slit widths totalling 20λ will provide singular detection of the desired maxima.

APPENDIX II

Determination of Slit Width of the Interferometer

In order to have the individual slits of the interferometer as wide as possible, for a low $a:d$ ratio, but at the same time narrow enough to prevent undue reflection from the sides of the channels, the following assumptions and determinations were made:

1. That the average monochromator exit slit width would be 500μ .
2. The length, L , of the interferometer, is equal to twice the focal length of the paraboloidal mirror, i. e., 49.5 approximates 2×26.7 .
3. Average width of channels, D , of the interferometer is 5 mm.

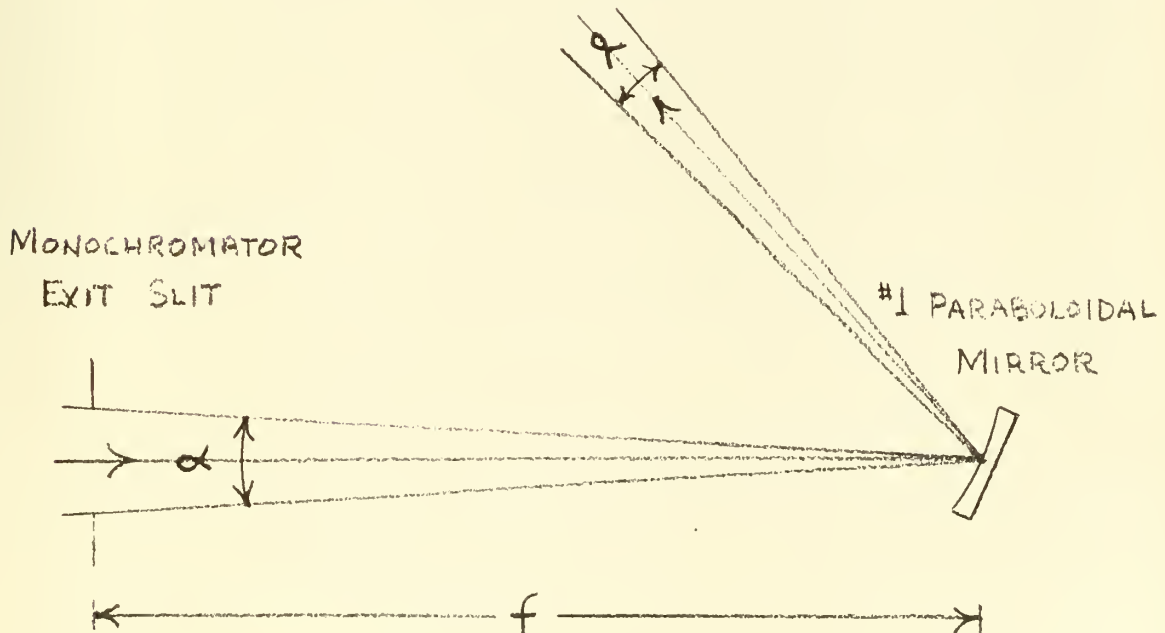


Figure 2. Divergence of Energy Due to Exit Slit Width



To determine optimum value of W:

$$\alpha = \frac{2W}{L} = \frac{g}{f}$$

but $L = 2f$, and $g = 0.5$ mm, therefore,

$$\frac{2W}{2f} = \frac{0.5}{f}$$

and width of slit of interferometer should be $D - 2W$ or
 $5 - 1 = 4$ mm.

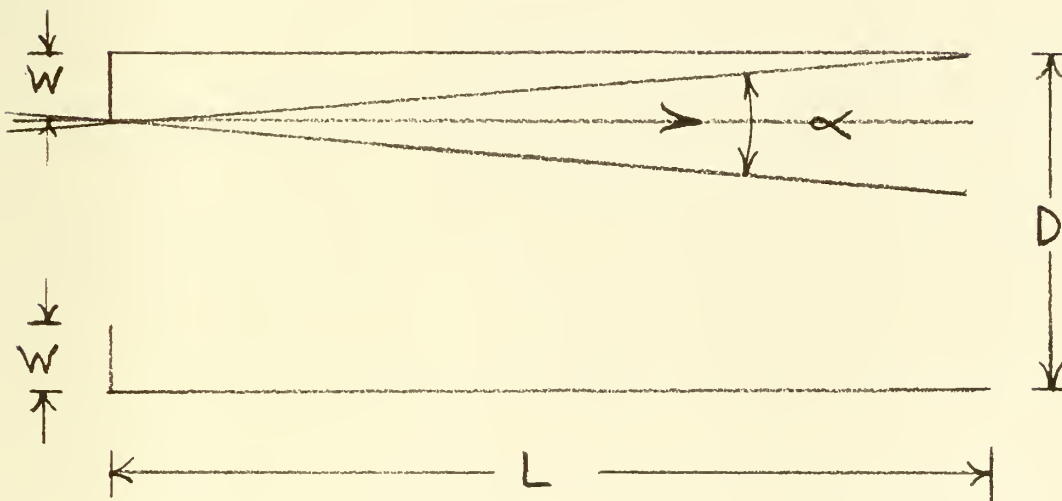


Figure 3. Effect of Divergence of Energy in Interferometer Channel

APPENDIX III

Determination of Amplitude Magnitude for Alternate Slit System

When the optical path through the vacuum channels of the interferometer and the gas filled channels differ by $m\lambda$, we have the standard six slit interference phenomenon with intensity of the pattern being governed by:

$$I = I_0 \frac{\sin^2 \beta}{\beta^2} \frac{\sin^2 N\gamma}{\sin^2 \gamma}$$

For simplification one may deal with amplitudes, for which the interference portion of the above expression would be

$$\frac{\sin N\gamma}{\sin \gamma}$$

which is derived as follows:

For two three slit systems (alternate slits of a six slit interferometer), we have:

$$\gamma = \frac{d \pi \sin \theta}{\lambda}$$

Since for alternate slits we have $2d$, then

$$2\gamma = \frac{2d \pi \sin \theta}{\lambda}$$

and

$$\frac{\sin 2\gamma}{\sin N 2\gamma} = \frac{\gamma_2 R_0}{\gamma_2 R_1}$$



or

$$R_1 = R_0 \frac{\sin N 2\gamma}{\sin 2\gamma} \quad \text{where } N = 3$$

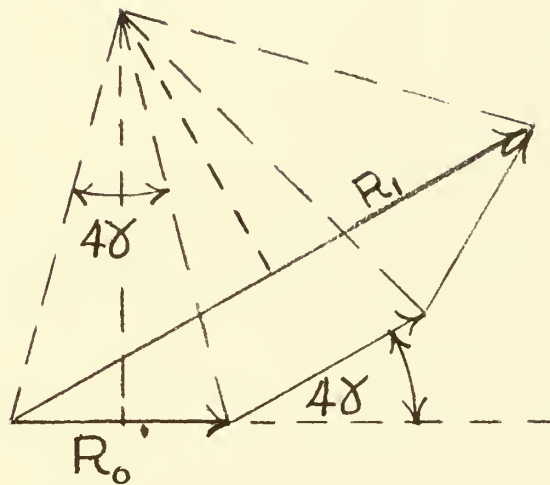


Figure 4. Phase Relationships of Three Alternate Slits

The second set of three slits will be at an angle 2γ from the first set so we have:

$$2R_1 \cos \gamma = R$$

Substituting for R_1 we have:

$$2R_0 \frac{\sin N 2\gamma}{\sin 2\gamma} \cos \gamma = R$$

Letting R_2 represent the resultant of the alternate channels filled by gas, we have:

$$R = 2 R_0 \frac{\sin N \gamma}{\sin 2 \gamma} \cos \frac{2 \gamma + \phi}{2}$$

where ϕ is the phase difference of R_2 caused by the gas.

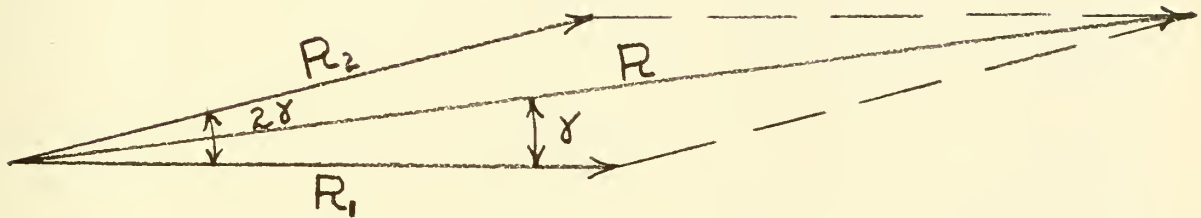


Figure 5. Phase Relationship of Alternate Groups of Three Slits

For a phase difference of ϕ equal to zero, and a trigonometric substitution of

$$\sin 2\gamma = 2 \sin \gamma \cos \gamma$$

we have:

$$R = R_0 \frac{\sin 6\gamma}{\sin \gamma}$$

which is the basic formula for a six slit interference pattern.

APPENDIX IV

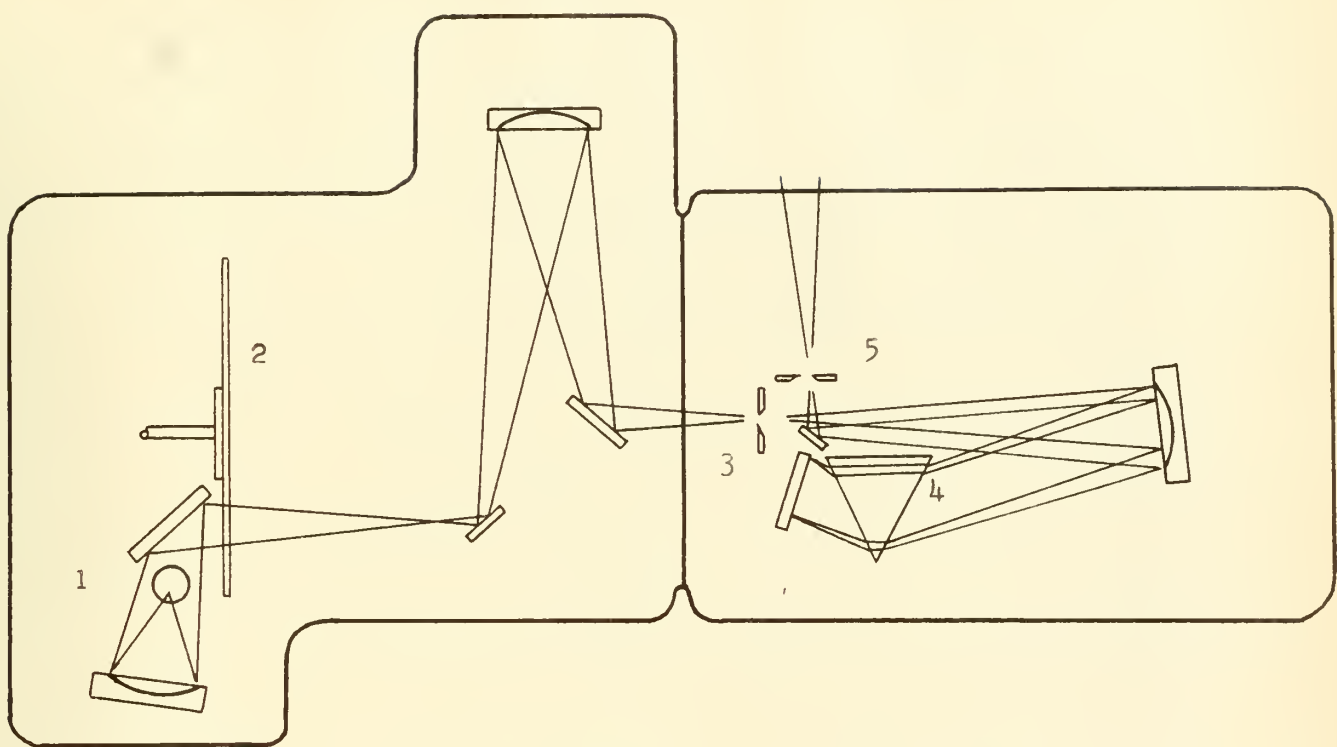


Figure 6. Infrared Source and Monochromator

Legend

1. Infrared Source (Nernst Glower)
2. Chopper
3. Entrance Slit
4. KBr Prism
5. Exit Slit



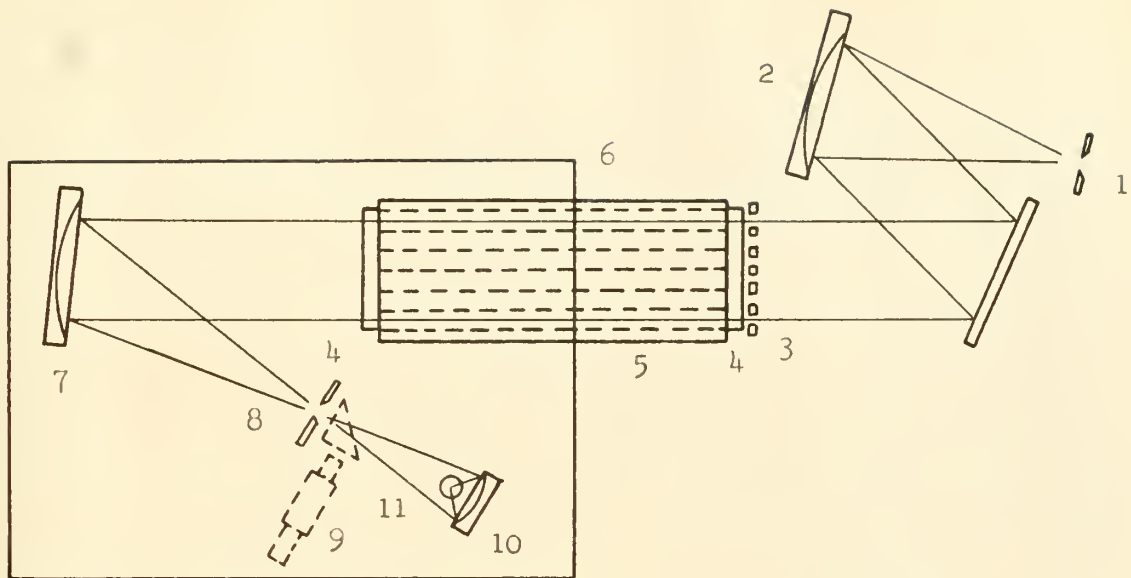


Figure 7. Interferometer Optical System

Legend

1. Monochromator Exit Slit
2. Off-axis Paraboloidal Collimating Mirror
3. Mask, Six Slits
4. KBr Windows
5. Modified Rayleigh Interferometer
6. Light Cover
7. Off-axis Paraboloidal Focusing Mirror
8. Detector Slit
9. Prism and Microscope (For Alignment Only)
10. Ellipsoidal Mirror
11. Thermocouple Detector

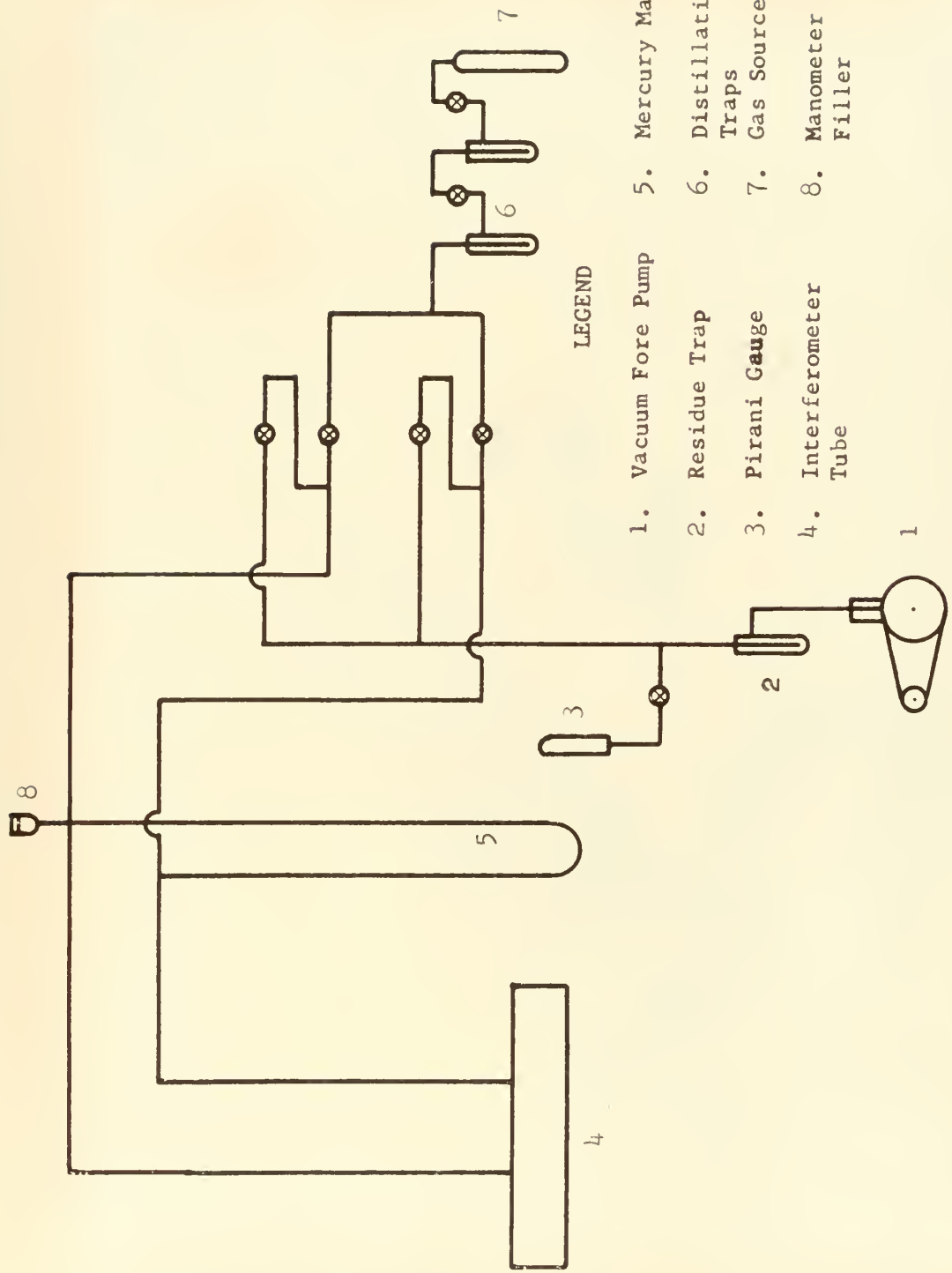


Figure 8. Vacuum and Distillation Systems



Figure 9. Modified Rayleigh Interferometer and Associated Components



Figure 10. Composite System with Light Covers Removed



Figure 11. Composite System with Light Covers Installed

thesE145
Design and construction of instrumentati



3 2768 001 90288 5

DUDLEY KNOX LIBRARY